Electronic Supplementary Information

Co-sputter Deposited Nickel-Copper Bimetallic Nanoalloy Embedded Carbon Films for Electrocatalytic Biomarker Detection

Shunsuke Shiba,[a,b,c] Dai Kato,[b] Tomoyuki Kamata[b,d] and Osamu Niwa[a,b]

a. Advanced Science Research Laboratory, Saitama Institute of Technology, Fusaiji, 1690, Fukaya, Saitama 369-0293, Japan.

b. National Institute of Advanced Industrial Science and Technology, 1-1-1, Higashi, Tsukuba, Ibaraki 305-8566, Japan.

c. Graduate School of Pure and Applied Sciences, University of Tsukuba, 1-1-1 Tennodai, Tsukuba, Ibaraki 305-8573, Japan.

d. Chiba Institute of Technology, 2-17-1, Tsudanuma, Narashino, Chiba 275-0016, Japan

E-mail: niwa@sit.ac.jp

Contents

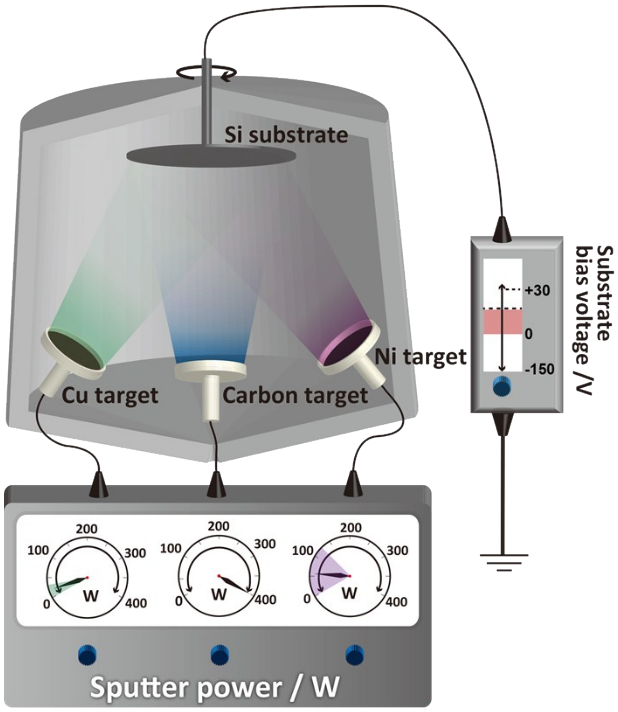

Fig. S1 The concept of UBM co-sputtering for fabricating nanoalloy embedded carbon film. This consists of carbon, Cu and Ni targets focused on the center of the substrate surface. This configuration and individually controlled system allows us to form the homogeneous films with a large area while controlling the compositions of the bimetallic nanoalloys in the film over a wide range. The UBM system also enables us to irradiate Ar ions during deposition, and its energy is controllable by changing the substrate bias voltage. This allows us to change the structure of the carbon film including the surface smoothness, its sp^2/sp^3 ratio, and possibly the ordering and size of the nanoalloys. Our method can fabricate an NP embedded structure by freely controlling the above parameters such as nanoalloy size, composition and surface roughness. This controllability is difficult to realize by similar co-sputtering system reported recently, where two targets of Ni-Cr alloy and silver were used to form the Ni-Cr nanoalloy embedded in Ag matrix (Bohra, M. et al., *Sci. Rep.*, **6**, 2016, 2045-2322).

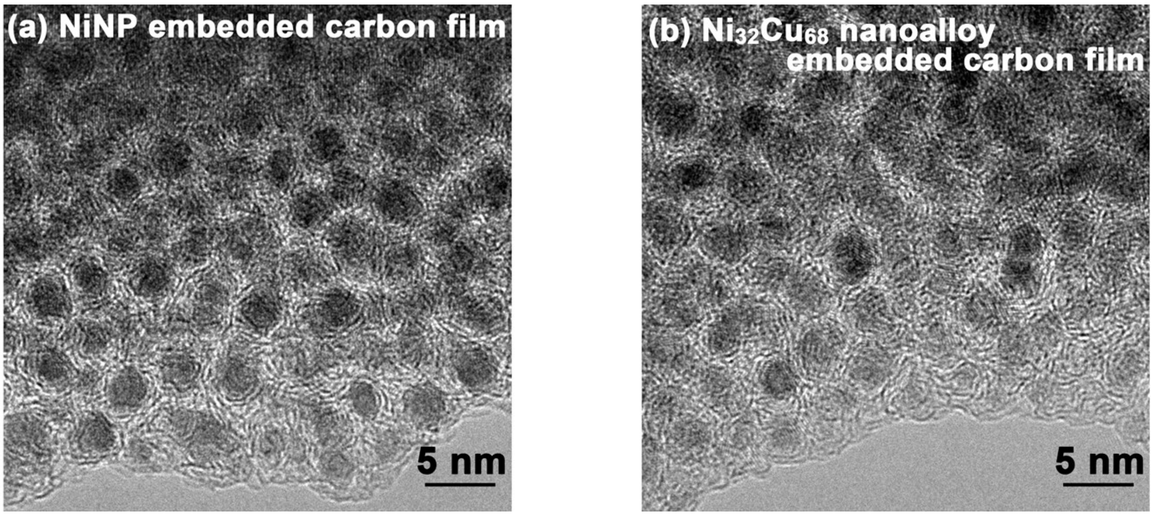

Fig. S2 HRTEM images of the (a) NiNP embedded carbon film and (b) $Ni_{32}Cu_{68}$ nanoalloy embedded carbon film. Atomic metal percentages and average diameter s of these films are summarized in Table 1.

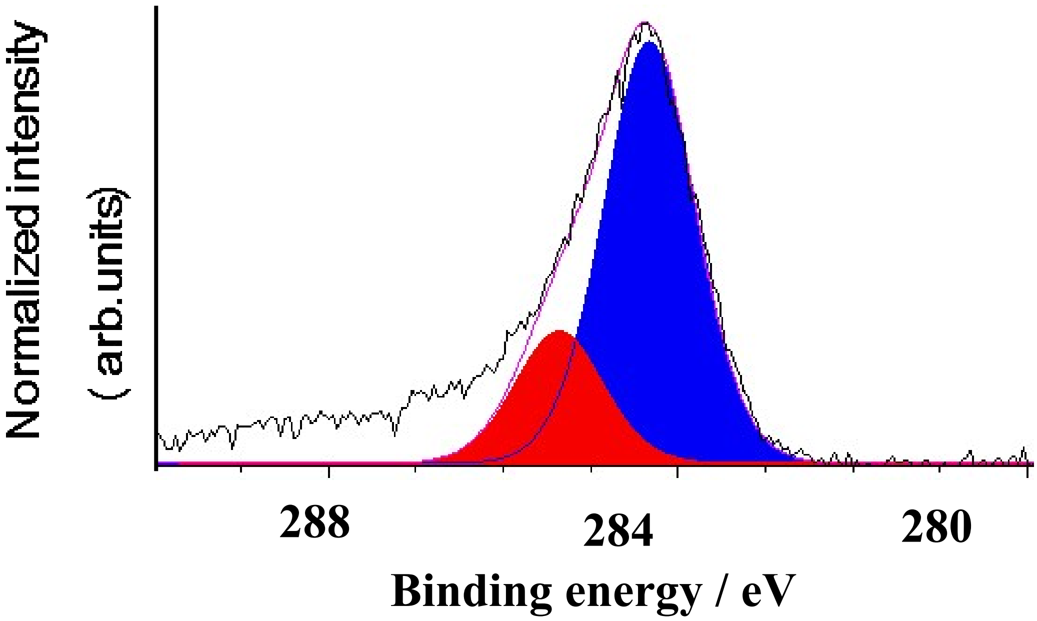

Fig. S3 High-resolution C 1s XPS spectra for $Ni_{61}Cu_{39}$ nanoalloy embedded carbon film. A Shimadzu/Kratos model AXIS Ultra (AlKα 1486.6 eV) spectrometer was used and the analysis was according to a previous report.[18] Each chemical bond ratio (sp^2/sp^3) was estimated using Shirley's method attributed to 284.5 eV for sp^2 bonds (blue) and 285.5 eV for sp^3 bonds (red).

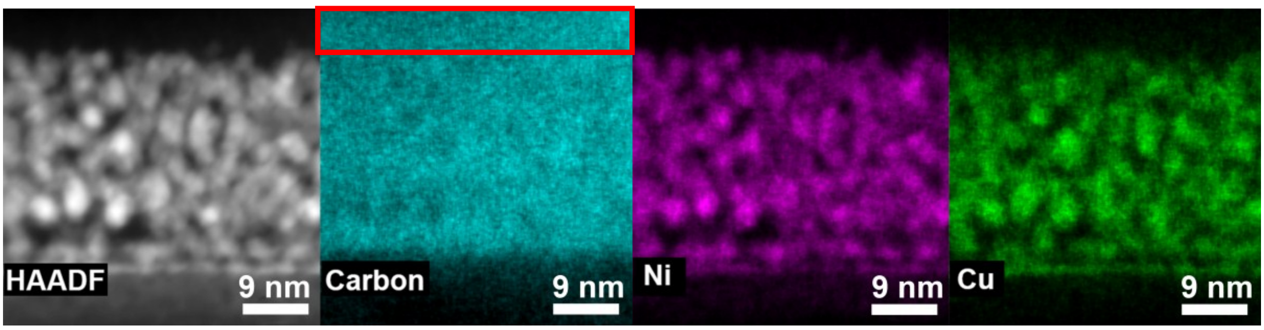

Fig. S4 The cross-sectional structure and elemental composition of the $Ni_{61}Cu_{39}$ nanoalloy embedded carbon film were investigated with an analytical transmission electron microscope (TEM), FEI Tecnai Osiris operated at 200 kV, equipped with an energy-dispersive X-ray spectrometer (EDS) and a high-angle annular dark-field scanning transmission electron microscopy (HAADF-STEM) system with a probe diameter of ~1 nm. Cross-sectional TEM samples were prepared using conventional mechanical polishing followed by argon ion milling. It should be noted that the EDS-mapped carbon located above the nanoalloys (corresponding to the red dotted rectangular region) were the signal from the epoxy resin used in the TEM observations.

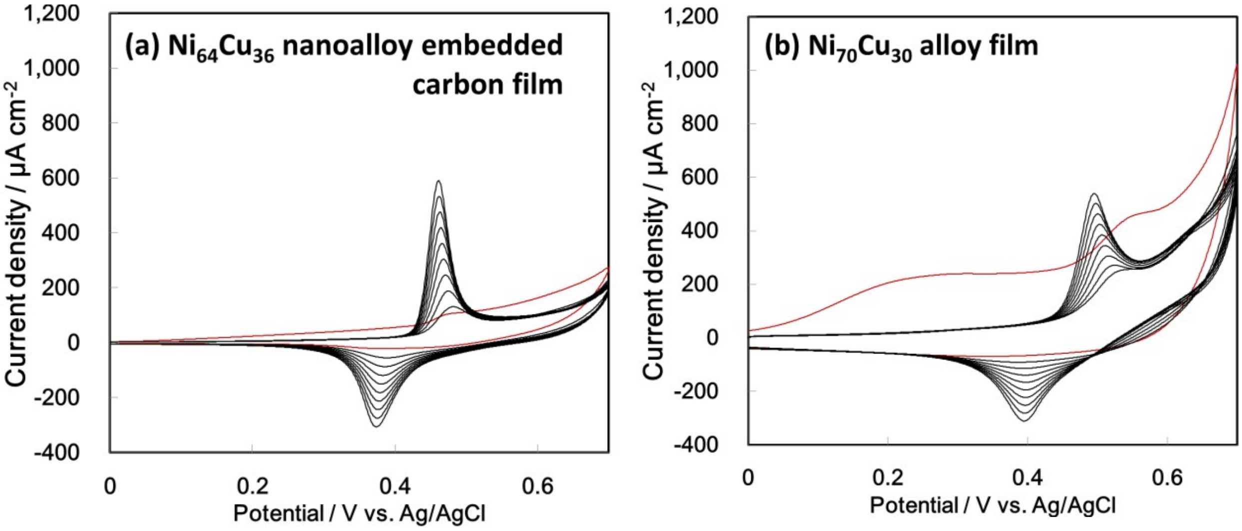

Fig. S5 Repeated CVs of (a) $Ni_{64}Cu_{36}$ nanoalloy embedded carbon film and (b) $Ni_{70}Cu_{30}$ alloy film obtained in 0.1 M NaOH solution. Red lines correspond to the first cycle and the other cycles are shown as black lines. Interestingly, the peak current of the nanoalloy exhibits a more negative potential and sharp shape than that of the alloy, the values at the 10^{th} cycle were 0.457 V for the nanoalloy and 0.495 V for the alloy. Moreover, the peak area for nanoalloy embedded carbon film at the 10^{th} cycle (89.1μC cm^{-2}) was larger than that of alloy film (83.6 μC cm^{-2}) despite the fact that the metal concentration was about 6 times smaller than that of alloy film. These results indicate that the nanoalloys embedded in carbon film have higher electrocatalytic activity than the alloy because more than 7 times the number of homogeneous active sites were formed at the lower potential.

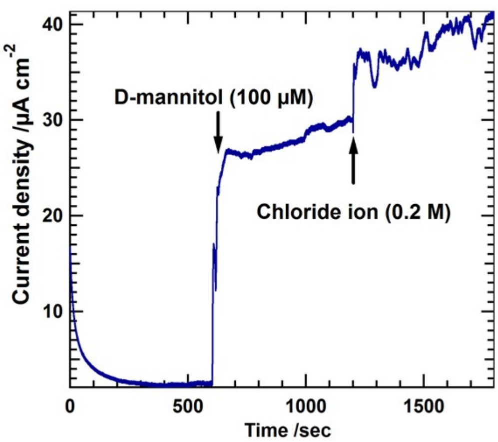

Fig. S6 Amperometric detection of D-mannitol obtained with $Ni_{64}Cu_{36}$ nanoalloy embedded carbon film electrode; NaOHaq, (0.1 M 0-600 s); D-mannitol (100 μM, 600-1200 s); D-mannitol (100 μM) in the presence of chloride ion (0.2 M, 1200-1800 s)

Layer	Target power /W C	Ni	Cu	Substrate bias voltage /V	Substrate rotated speed /rpm	Background pressure /Pa	Ar pressure (working pressure) /Pa	Ar flow rate / sccm	Deposition time /s	XPS results (Ni+Cu) at. %	XPS results Ni/Cu	Average diameter /nm
a	400	28	8	-20 V	60	< 1.0 ×10^{-6} Pa	0.6	15	100	12.0	55/45	2.7
b	401	0	0						180	-	-	-
c	400	81	0						240	18.7	100/0	3.6
d	400	0	0						180	-	-	-
e	400	28	0						270	8.7	100/0	2.5
f	400	0	0						120	-	0	-

Table S1. Sputter conditions for each layer in the stepwise deposited film and the properties of the nanoalloys

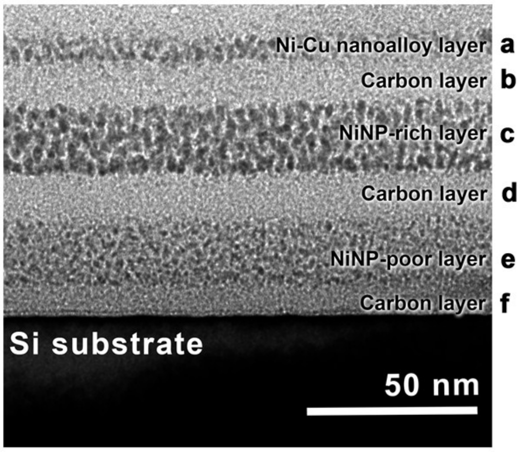

Table S2. Sputter conditions and XPS results for the resultant films

Target power /W C	Ni	Cu	Substrate bias voltage /V	Substrate rotated speed /rpm	Background pressure /Pa	Ar pressure (working pressure) /Pa	Ar flow rate / sccm	Deposition time /s	XPS results (Ni+Cu) at. %	XPS results Ni/Cu	Use this electrode at:
400	112	0	-20 V	60	< 1.0 ×10^{-6} Pa	0.6	15	360	14.7	100/0	Fig. 3(c)
401	79	10						360	15.6	64/36	Fig. 3(a,c,d)
400	69	13						344	14.0	61/39	Fig. 2
400	57	17						360	15.3	41/59	Fig. 3(c)
400	35	22						360	15.5	32/68	Fig. S2
400	24	25						400	18.7	26/74	Fig. 3(c)
401	0	30						360	16.9	0/100	Fig. 3(c)
0	68	13						2640	100 (only	70/30	Fig. 3(b), Fig. S5(b)

*Si substrate are used after blowing N_2 gas.

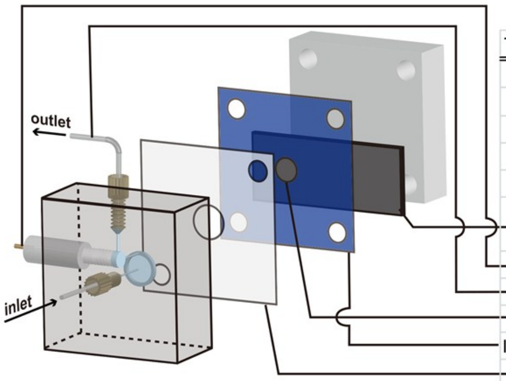

Table S3. Conditions for the continuous flow measurements using radial flow cell.

Pretreatment	Applied 0.5 V for 30 min
Applied potential	0.5 V
Volume flow rate	0.2 mL/min
Mobile phase	NaOH solution (50 mM)
Analyte	D-mannitol (100 μM)
Working electrode	(a)$Ni_{64}Cu_{36}$ nanoalloy embedded carbon film (b)$Ni_{70}Cu_{30}$ alloy film
Reference electrode	Ag/AgCl
Counter	SUS pipe
electrode area	0.126 cm^2 (4 mm diameter)
Insulating tape thickness	80 μm
gasket thickness	25 μm